Active Steering and Anti-Roll Shared Control for Enhancing Roll Stability in Path Following of Autonomous Heavy Vehicle

Conference Paper *in* SAE Technical Papers · April 2019

DOI: 10.4271/2019-01-0454

CITATIONS
8

READS
629

4 authors:

Liu Yulong
Tsinghua University
27 PUBLICATIONS **559** CITATIONS
SEE PROFILE

Kaiming Yang
Tsinghua University
55 PUBLICATIONS **782** CITATIONS
SEE PROFILE

Xiangkun He
University of Electronic Science and Technology of China
68 PUBLICATIONS **1,417** CITATIONS
SEE PROFILE

Xuewu Ji
Tsinghua University
90 PUBLICATIONS **1,794** CITATIONS
SEE PROFILE

2019-01-0454 Published 02 Apr 2019

Active Steering and Anti-Roll Shared Control for Enhancing Roll Stability in Path Following of Autonomous Heavy Vehicle

Yulong Liu, Kaiming Yang, Xiangkun He, and Xuewu Ji Tsinghua University

Citation: Liu, Y., Yang, K., He, X., and Ji, X., "Active Steering and Anti-Roll Shared Control for Enhancing Roll Stability in Path Following of Autonomous Heavy Vehicle," SAE Technical Paper 2019-01-0454, 2019, doi:10.4271/2019-01-0454.

Abstract

Rollover accident of heavy vehicle during cornering is a serious road safety problem worldwide. In the past decade, based on the active intervention into the heavy vehicle roll dynamics method, researches have proposed effective anti-roll control schemes to guarantee roll stability during cornering. Among those studies, however, roll stability control strategies are generally derived independent of front steering control inputs, the interactive control characteristic between steering and anti-roll system have not been thoroughly investigated. In this paper, a novel roll stability control structure that considers the interaction between steering and anti-roll system, is presented and discussed. The proposed control framework is implemented based on dynamic game theory in which heavy vehicle roll stability can be represented as a dynamic difference game so that its two players, namely the active steering (AS) and active anti-roll bar (AARB) system, can work together to provide more roll stability to the heavy vehicle system during cornering. The interactive control strategy between AS and AARB system is obtained by non-cooperative closed-loop feedback Nash game equilibrium theory to ensure optimal roll stability performance. In order to validate the effectiveness of proposed control strategy in a more comprehensive way, a H_∞ optimal roll stability control strategy in which the input of AS is only regarded as the exogenous disturbance, is also presented and used as comparison. Simulation results of double lane change (DLC) maneuver show that the proposed AS-AARB shared control strategy can significantly improve the roll stability as well as lateral stability while ensure desired path tracking performance during cornering.

Introduction

Rollover is a common accident among heavy commercial vehicles which usually cause severe consequences such as large financial costs as well as personal injuries and fatalities [1, 2]. Compared with passenger cars, heavy vehicles are prone to lose roll stability during cornering and lane changing due to their high situated center of gravity (CoG) in proportion to track widths [3]. Besides the passive anti-roll bars which have been equipped on most heavy vehicle, several active anti-roll control schemes concerning with the improvement of roll stability, such as active suspension control [3], active steering [4] and active braking [5], are proposed and discussed in the literatures.

S. Yim *et al* [6] propose a linear quadratic (LQ) static output feedback (SOF) control strategy for designing the active anti-roll controller that uses the AARB and electronic stability program (ESP), simulation results show that the proposed method is effective in preventing rollover. Gaspar *et al.* [7] design a combined control structure to prevent the rollover of heavy vehicle, LPV controller synthesis approach is used to schedule the control inputs of AARB and active braking system. M. Ghazali *et al.* [8] propose the hierarchy control strategy to investigate the path following in the presence of rollover risk. The MPC based steering controller is designed to guarantee the roll stability and the interconnection between brake and steering controller is reflected in the upper layer controller (ULC) indirectly, simulation results show that such multilayer control framework maintains roll stability while path tracking error is guaranteed. In [9], introducing the AARB made of four electronic servo-valve hydraulic actuators, the active anti-roll control is achieved by solving a LQ optimization control problem in which the front steering input is regarded as uncertain disturbance, both frequency and time domains simulation results show that the proposed control strategy significantly improve the roll stability.

Whereas, these researches generally design the active anti-roll control strategy by regarding the steering inputs as exogenous disturbances [6, 7, 8, 9], without making adequate investigation of the interactive control characteristic between the steering and anti-roll control. Dynamic game theory, which has potential application in control design in situations with optimization behavior and multiple decision-makers [10], provides the systematic design framework for such shared control problem.

Remark 1: In order to improve the intelligent level of heavy vehicle, a more intelligent steering system which can

FIGURE 1 Electrically assisted hydraulic steering [11].

realize the function of active steering is needed. By integrating a small electro-mechanic actuator into the HPS system (as shown in Fig. 1), the autonomous steering (AS) can be realized in an easy way [11].

In the past decade, the dynamic game theory has received wide attention in modelling and investigating the conflicts which involve multiple player/agents and optimization behavior. Clement D. *et al* [12] applied the Stackelberg equilibrium game theory to develop and validate an energy management controller for hybrid electric vehicles (HEVs). Based on open-loop and closed-loop feedback Nash or Stackelberg equilibrium theory, the interactive steering control strategies between human driver and active steering system (AFS) have been derived and investigated in [13, 14]. X. Ji *et al* [15] proposed the interactive control-based robust lateral stability control method to design the autonomous automobile path tracking controller and two agents are AFS and active rear steering (ARS) system. However, to the best of the authors knowledge, such dynamic game theory-based interactive control concept has not been applied to design the active anti-roll control strategy for heavy vehicle.

In this paper, a novel roll stability controller design framework for heavy vehicle path following, namely dynamic game theory-based path following - active anti-roll (AAR) interactive shared control strategy, is proposed and discussed. In the process of cooperative path following-roll stability control, the control strategies of two players, namely AS and AARB system, are obtained by closed-loop feedback Nash equilibrium theory to ensure the optimal performance. Furthermore, in order to validate the effectiveness of the proposed interactive path following-AAR control strategy in a more comprehensive way, a H_∞ optimal roll stability controller in which steering angle is only considered as the uncertain disturbance, is also designed and used as comparison. Finally, Simulation of various driving scenarios are carried out to verify the effectiveness of the proposed roll stability control strategy.

The remainder of the paper is organized as follows. Firstly, the yaw-roll model of single unit heavy vehicle and closed-loop feedback Nash equilibrium theory-based path following-AAR interactive control strategy are discussed. And then based on the yaw-roll model a H_∞ optimal roll stability controller, which served as a contrast, is introduced. Finally, cases studies are provided where simulation results of DLC driving scenarios are presented and analyzed. Simulation results show that the proposed control framework can significantly enhance vehicle stability (roll stability as well as lateral stability) meanwhile provide enhanced path tracking performance.

AS and AARB Shared Control of Path Following-Roll Stability for Heavy Vehicle

In order to derive the following AS and AARB shared path following-roll stability control for heavy vehicle, a sixth-order linear single unit heavy vehicle model with coupled yaw-roll dynamics and optimal linear preview path following model are presented firstly.

Heavy Vehicle Combined Yaw-Roll Dynamics and Optimal Preview Path Following Control

For roll stability study, only lateral, yaw and roll dynamics are reserved in the simplified linear model. The assumptions of instantaneously constant longitudinal speed and linear tyre model are necessary before constructing the linear vehicle model [16]. Fig. 2 illustrates the combined yaw-roll dynamics of heavy vehicle modelled by a three-body system, in which m_s is the sprung mass, m_{uf} is the unsprung mass at the front including the front wheel and axle, m_{ur} is the unsprung mass at the rear including the rear wheel and axle. The notations of yaw-roll model can be found in Table I.

In order to improve the roll stability of heavy vehicle, the active anti-roll bars (AARB) system is adopted to generate a stabilizing moment to balance the destabilizing overturning moment. The basic operation principle of this system is: four electronic servo-valve hydraulic dampers can be controlled by electric current signals and then the hydraulic damping force will be generated. Based on these damping forces, the active anti-roll torque T_f and T_r will be exerted on the front and rear axle, respectively. The more detailed description about this system can be found in [3].

FIGURE 2 Yaw-roll model of single unit heavy vehicle [3,7].

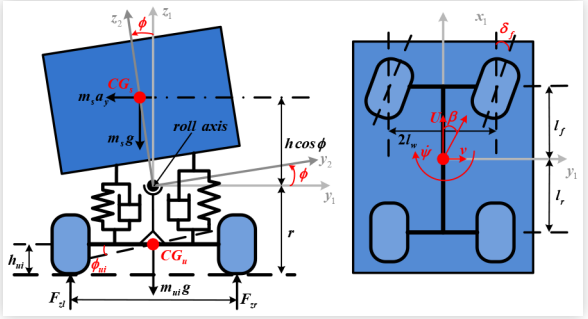

TABLE 1 Notations of the yaw-roll model [6, 7].

Notation	Description
m_s	Sprung mass
m_{uf}	Unsprung mass at the front axle
m_{ur}	Unsprung mass at the rear axle
m	Total vehicle mass
U	Forward velocity
h	Height of CG of sprung mass from roll axis
h_u	Height of CG of unsprung mass from ground
r	Height of roll axis from ground
a_y	Lateral acceleration
β	Side-slip angle at the center of mass
$\dot{\psi}$	Yaw rate
ϕ	Sprung mass roll angle
ϕ_{uf}	Unsprung mass roll angle at the front axle
ϕ_{ur}	Unsprung mass roll angle at the rear axle
δ	Steering angle
C_f	Tyre cornering stiffness at the front axle
C_r	Tyre cornering stiffness at the rear axle
k_f	Suspension roll stiffness at the front axle
k_r	Suspension roll stiffness at the rear axle
b_f	Suspension roll damping at the front axle
b_r	Suspension roll damping at the rear axle
k_{tf}	Tyre roll stiffness at the front axle
k_{tr}	Tyre roll stiffness at the rear axle
I_{xx}	Roll moment of the inertia of sprung mass
I_{xz}	Yaw-roll product of inertia of sprung mass
I_{zz}	Yaw moment of inertia of sprung mass
l_f	Length of the front axle from the CG
l_r	Length of the rear axle from the CG
l_w	Half of the vehicle width
g	Gravity of earth
T_f	Control torque at the front axle
T_r	Control torque at the rear axle

As a whole system, heavy vehicle can translate laterally and exhibit yaw motion. In vehicle modelling, the motion differential equations of the yaw-roll dynamics of the single unit heavy vehicle are formalized, that is, the lateral dynamics, the yaw moment, the roll moment of the sprung mass, the roll moment of the front and the rear unsprung masses.

$$mU\dot{\beta} - m_s h\ddot{\phi} = Y_\beta \beta + Y_{\dot{\psi}}\dot{\psi} + Y_\delta \delta \tag{1}$$

$$-I_{xz}\ddot{\phi} + I_{zz}\ddot{\psi} = N_\beta \beta + N_{\dot{\psi}}\dot{\psi} + N_\delta \delta \tag{2}$$

$$\begin{aligned}&\left(I_{xx} + m_s h^2\right)\ddot{\phi} - I_{xz}\ddot{\psi} = m_s g h\phi + m_s U h\left(\dot{\beta} + \dot{\psi}\right)\\ &-k_f\left(\phi - \phi_{uf}\right) - b_f\left(\dot{\phi} - \dot{\phi}_{uf}\right) - k_r\left(\phi - \phi_{ur}\right)\\ &-b_r\left(\dot{\phi} - \dot{\phi}_{ur}\right) + T_f + T_r\end{aligned} \tag{3}$$

$$\begin{aligned}&-rC_f\left(-\beta + \delta - \frac{l_f\dot{\psi}}{U}\right) = m_{uf}U\left(r - h_{uf}\right)\left(\dot{\beta} + \dot{\psi}\right)\\ &+m_{uf}gh_{uf}\phi_{uf} - k_{tf}\phi_{uf} + k_f\left(\phi - \phi_{uf}\right) + b_f\left(\dot{\phi} - \dot{\phi}_{uf}\right) + T_f\end{aligned} \tag{4}$$

$$\begin{aligned}&-rC_f\left(-\beta + \frac{l_f\dot{\psi}}{U}\right) = m_{ur}U\left(r - h_{ur}\right)\left(\dot{\beta} + \dot{\psi}\right)\\ &-m_{ur}gh_{ur}\phi_{ur} - k_{tr}\phi_{ur} + k_r\left(\phi - \phi_{ur}\right) + b_r\left(\dot{\phi} - \dot{\phi}_{ur}\right) + T_r\end{aligned} \tag{5}$$

where

$$Y_\beta = -\left(C_f + C_r\right), Y_{\dot{\psi}} = -mU + \frac{C_r l_r - C_f l_f}{U}, Y_\delta = C_f$$

$$N_\beta = C_r l_r - C_f l_f, N_{\dot{\psi}} = -\frac{C_r l_r^2 + C_f l_f^2}{U}, N_\delta = C_f l_f$$

Defining the state vector

$$\mathbf{x}_v = \left[\beta \;\; \dot{\psi} \;\; \phi \;\; \phi_{uf} \;\; \phi_{ur} \;\; \dot{\phi}\right]^T_{6\times 1}$$

Equations (1)-(5) can be expressed in the linear time-invariant (LTI) state-space representation as

$$\dot{\mathbf{x}}_v = \mathbf{A}_v\mathbf{x}_v + \hat{\mathbf{B}}_\delta\delta + \hat{\mathbf{B}}_\mathbf{T}\mathbf{T} \tag{6}$$

Where A_v, $\hat{B}_\delta$, $\hat{B}_T$ are model matrices of appropriate dimensions. The matrices A_v, $\hat{B}_\delta$, $\hat{B}_T$ are shown in Appendix.

And next, the kinematic states of heavy vehicle, such as global lateral displacement and yaw angle, should be given. The yaw angle can be obtained by integration of yaw rate and the global lateral displacement of heavy vehicle can be obtained by integration of Equation (7)

$$\dot{y} = U\left(\sin\psi + \beta\cos\psi\right) \tag{7}$$

Assumping small yaw displacement as in [14], Equation (7) can be reduced to

$$\dot{y} = U\left(\psi + \beta\right) \tag{8}$$

Combined with (6), the dynamical equation of the yaw-roll heavy vehicle model can be augmented as follows

$$\dot{\mathbf{x}}_c = \mathbf{A}_\mathbf{c}\mathbf{x}_\mathbf{c} + \mathbf{B}^\mathbf{c}_\delta\delta + \mathbf{B}^\mathbf{c}_\mathbf{T}\mathbf{T} \tag{9}$$

where $\mathbf{x_c}$ is the augmented system state and

$$\mathbf{A}_\mathbf{c} = \begin{bmatrix}\mathbf{A_v} & \mathbf{0}_{6\times 2}\\ \upsilon_1 & \upsilon_2\end{bmatrix}, \upsilon_1 = \begin{bmatrix}U & 0 & \mathbf{0}_{1\times 4}\\ 0 & 1 & \mathbf{0}_{1\times 4}\end{bmatrix}, \upsilon_2 = \begin{bmatrix}0 & U\\ 0 & 0\end{bmatrix}$$

$$\mathbf{B}^\mathbf{c}_\delta = \begin{bmatrix}\hat{B}_\delta\\ \mathbf{0}_{2\times 1}\end{bmatrix}, \mathbf{B}^\mathbf{c}_\mathbf{T} = \begin{bmatrix}\hat{B}_T\\ \mathbf{0}_{2\times 2}\end{bmatrix}$$

$$\mathbf{x}_\mathbf{c} = \begin{bmatrix}\beta & \dot{\psi} & \phi & \phi_{uf} & \phi_{ur} & \dot{\phi} & y & \psi\end{bmatrix}^T_{8\times 1}$$

In order to facilitate the following path tracking control design, using the MATLAB function "c2d", the discretization form of (9) can be obtained as

$$\mathbf{x}\left(k+1\right) = \mathbf{A}\mathbf{x}\left(k\right) + \mathbf{B}_\delta\delta\left(k\right) + \mathbf{B}_\mathbf{T}\mathbf{T}\left(k\right) \tag{10}$$

where $\mathbf{x}$(k) and $\mathbf{x}$(k+1) represent the discrete state of (9) for current and next time step, respectively.

By integrating the electro-mechanic actuator into the HPS system, the autonomous steering function of heavy vehicle can be achieved. In this paper, we are not intended to give more concerns about the modelling or control of such electrically assisted hydraulic steering system, it is assumed

that the front wheel can be controlled directly by the upper path tracking controller.

To facilitate the following controller design, the linear quadratic optimization-based path following control is introduced and discussed. The more detailed introduction about this path tracking control strategy can be found in [16].

Firstly, using the concept of "shift register" [16], the updating of steering controller's road path preview can be represented as

$$\mathbf{R}_{as}(k+1)=\boldsymbol{\kappa}\mathbf{R}_{as}(k)+\Delta\mathbf{r}_{as}^{updata} \tag{11}$$

where

$$\mathbf{R}_{as}(k)=\begin{bmatrix}\mathbf{r}_{as}(k)\\ \mathbf{r}_{as}(k+1)\\ \mathbf{r}_{as}(k+2)\\ \vdots\\ \mathbf{r}_{as}(k+N_p-1)\\ \mathbf{r}_{as}(k+N_p)\end{bmatrix},\quad \boldsymbol{\kappa}=\begin{bmatrix}0&1&0&0&\cdots&0\\ 0&0&1&0&\cdots&0\\ 0&0&0&1&\cdots&0\\ \vdots&\vdots&\vdots&\vdots&\ddots&\vdots\\ 0&0&0&0&0&1\\ 0&0&0&0&0&0\end{bmatrix},$$

$$\Delta=\begin{bmatrix}0&0&0&\cdots&0&1\end{bmatrix}^T,\mathbf{r}_{as}^{updata}=\mathbf{r}_{as}(k+N_p+1)$$

where k denotes the discrete-time index, taking values in the set of integers:$\mathbf{K}:=\{1,2,\cdots N_p\}$,$\mathbf{r}_{as}(k)$consists of two elements: Desired lateral displacement $r_{as}^{y}(k)$ and yaw angle $r_{as}^{\psi}(k)$ of steering system. Namely, $\mathbf{r}_{as}(k)=\begin{bmatrix}r_{as}^{y}(k) & r_{as}^{\psi}(k)\end{bmatrix}^T$. N_p is the preview horizon. At an instant k, the sample value $\mathbf{r}_{as}(k+h)$ $(1\le h\le N_p)$ becomes $\mathbf{r}_{as}(k+h-1)$; at instant $(k+1)$, $\mathbf{r}_{as}^{updata}$ is viewed as a new value, and enters $\mathbf{r}_{as}(k+N_p)$, it is convenient to regard this as the single external input to the system and to regard others $(k+N_p)$ sample values as system states.

Then, by removing the $\mathbf{B_T T}(k)$ in Equation (10) and combining this new discrete-time heavy vehicle linear yaw-roll model with road preview information (11), the combination of the road path information of steering system and discrete time vehicle equation can be formalized as

$$\boldsymbol{\Psi}_{as}(k+1)=\mathbf{A}_{\Gamma}^{as}\boldsymbol{\Psi}_{AFS}(k)+\mathbf{B}_{\Gamma}^{as}\delta(k)+\Delta_{\Gamma}^{as}\mathbf{r}_{as}^{updata} \tag{12}$$

where

$$\boldsymbol{\Psi}_{as}(k)=\begin{bmatrix}\mathbf{x}(k)\\ \mathbf{R}_{as}(k)\end{bmatrix},\mathbf{A}_{\Gamma}^{as}=\begin{bmatrix}\mathbf{A}&\mathbf{0}\\ \mathbf{0}&\rho\end{bmatrix},\mathbf{B}_{\Gamma}^{as}=\begin{bmatrix}\mathbf{B}_{\delta}\\ \mathbf{0}\end{bmatrix},\Delta_{\Gamma}^{as}=\begin{bmatrix}\mathbf{0}\\ \Delta\end{bmatrix}$$

Next, as illustrated in [16], a quadratic cost function g_s should be given to evaluate the path tracking performance over N_p future time steps

$$g_{as}(N_p,k)=\frac{1}{2}\sum_{l=0}^{N_p}\left[\boldsymbol{\Psi}_{as}^{T}(k+l)\boldsymbol{\xi}_{as}\boldsymbol{\Psi}_{as}(k+l)+\delta(k)\mathbf{R}_{as}^{input}\delta(k)\right] \tag{13}$$

where

$$\boldsymbol{\xi}_{as}=\mathbf{H}_{as}^{T}\mathbf{Q}_{as}\mathbf{H}_{as},\mathbf{Q}_{as}=diag\begin{pmatrix}q_{as}^{v} & q_{as}^{\omega} & q_{as}^{y} & q_{as}^{yaw}\end{pmatrix},\mathbf{R}_{as}^{input}=\begin{bmatrix}r_{as}^{input}\end{bmatrix}$$

$$\mathbf{H}_{as}=\begin{bmatrix}1&0&\mathbf{0}_{1\times5}&0&0&1/T_s&0&1/T_s&0&\cdots&0\\ 0&1&\mathbf{0}_{1\times5}&0&0&0&1/T_s&0&1/T_s&\cdots&0\\ 0&0&\mathbf{0}_{1\times5}&1&0&-1&0&0&0&\cdots&0\\ 0&0&\mathbf{0}_{1\times5}&0&-1&0&-1&0&0&\cdots&0\end{bmatrix}_{4\times(8+2N_p)}$$

$\boldsymbol{\xi}_{as}$ and $\mathbf{R}_{as}^{input}$ are the path following error weighing matrix and the input weight matrix, respectively; $\mathbf{Q}_{as}$ is a matrix used to weight the specific index of path following effect and the relative importance attached to lateral velocity, yaw rate, lateral displacement and yaw angle, which are set by choosing q_{as}^{v}, q_{as}^{ω}, q_{as}^{y} and q_{as}^{ψ} appropriately.

Finally, based on the principle of minimum, the optimal steering control for heavy vehicle path tracking can be obtained by solving the following dynamic quadratic optimization problem

$$\begin{aligned}&\delta^{*}(k)=\arg\min_{\delta(k)\in\boldsymbol{\kappa}(k)}g_{as}\left(N_p,k,\delta(k),\boldsymbol{\Psi}_{as}^{*}(k)\right)\\ &s.t.\ \ \boldsymbol{\Psi}_{as}^{*}(k+1)=\mathbf{A}_{\Gamma}^{as}\boldsymbol{\Psi}_{as}^{*}(k)+\mathbf{B}_{\Gamma}^{as}\delta(k)+\Delta_{\Gamma}^{as}\mathbf{r}_{as}^{updata},\\ &\boldsymbol{\Psi}_{as}^{*}(0)=\boldsymbol{\Psi}_{as}(0)\end{aligned} \tag{14}$$

AS and AARB Shared Control of Path Following-Roll Stability for Heavy Vehicle

Heavy vehicle cornering is one of the most dangerous maneuvers due to the fact that the loss of control (rollover or lateral stability) of heavy vehicle may be more prone to occur in such driving scenario. It can be naturally deduced that in the progress of vehicle path following, human driver mainly aims to improve the accuracy of path tracking (e.g., minimize the lateral offset) while without fully consideration to roll stability, or in other words, the optimization objectives or interests of AS system and AARB system may conflict with each other's, so unlike most paper on vehicle path tracking or roll stability subject, we treat not only path tracking accuracy but also vehicle roll stability in the optimization directly.

Using dynamic game theory, the shared control strategy of path following-AAR for heavy vehicle can be developed, and the AS and AARB are defined as two players in the dynamic game system.

As illustrated in [3], the control objective of AARB system is to maximize the roll stability of the heavy vehicle. The most direct and interest performance characteristics for roll stability controller design are the normalized load transfer at the front and rear axles, which can be described as

$$N_f=\frac{\Delta F_{zf}}{F_{zf}},\ N_r=\frac{\Delta F_{zr}}{F_{zr}} \tag{15}$$

where F_{zf} and F_{zr} are the total axle load at the front and rear axle, respectively. $\Delta F_{zf}$and$\Delta F_{zr}$are, respective, the lateral load transfers at the front and rear axles, which can be given as [3]

$$F_{zf}=\frac{l_r}{l_f+l_r}mg,F_{zr}=\frac{l_f}{l_f+l_r}mg,\Delta F_{zf}=\frac{k_{tf}\phi_{uf}}{l_w},\Delta F_{zr}=\frac{k_{tr}\phi_{ur}}{l_w} \tag{16}$$

The values of N_f and N_r correspond to the largest possible load transfer. Furthermore, while attempting to minimize the normalized load transfer at the front and rear axles, other variables of interest to be optimized such as sprung mass roll angle ϕ, the roll angles between the sprung and unsprung masses $(\phi-\phi_{uf,r})$, the control inputs of active anti-roll torques $T_{f,r}$ should also be considered in the synthesis of roll stability controller.

FIGURE 3 Interactive path following-AAR control paradigm

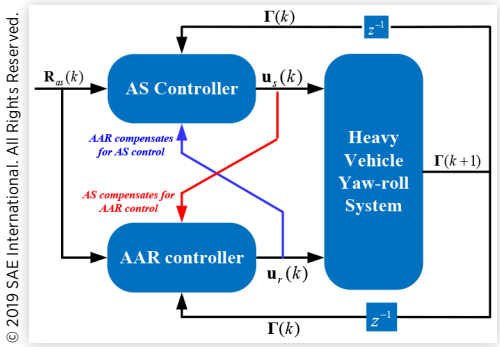

In this paper, the path following-AAR shared control strategy for heavy vehicle is constructed as a non-cooperative closed-loop feedback Nash equilibrium game between AS and AARB, with the costs penalizing the indexes of path tracking accuracy (e.g., lateral offset), lateral stability (e.g., lateral velocity) as well as roll stability (e.g., normalized load transfer). Fig. 3 shows the interactive path following-AAR control paradigm.

Remark 2: Unlike passenger cars, loss of yaw stability like spin-out or side-slide is a common safety issue. Heavy vehicle tends to loss roll stability as a result of its high center of gravity (CG) to track-width ratio and normal tyre forces [18]. Consider the fact that nonlinear behavior of vehicle lateral dynamic mainly results from tyre lateral nonlinearity and heavy vehicle may behave more linear in tyre compared with passenger cars, so linear quadratic (LQ) dynamic game theory provides a very suitable framework to investigate the interactive roll stability control problem for heavy vehicle.

Consider the interactive path following-AAR control framework, augmenting Equation (12) with AAR control inputs, the "path following-AAR global system" equation can be obtained as

$$\mathbf{\Psi}(k+1)=\mathbf{A}_x\mathbf{\Psi}(k)+\mathbf{B}_s\mathbf{u}_s(k)+\mathbf{B}_r\mathbf{u}_r(k)+\Delta_x^s\mathbf{r}_{as}^{updata} \quad (17)$$

where

$$\mathbf{\Psi}(k)=\mathbf{\Psi}_{as}(k),\mathbf{A}_x=\mathbf{A}_\Gamma^{as},\mathbf{B}_s=\mathbf{B}_\Gamma^{as},\mathbf{u}_s(k)=\delta(k),$$
$$\mathbf{u}_r(k)=\mathbf{T}(k),\Delta_s^s=\Delta_\Gamma^{as},\mathbf{B}_r=\begin{bmatrix}\mathbf{B}_\mathbf{T}^T & \mathbf{0}_{1\times 2N_p}\end{bmatrix}^T$$

In order to derive the interactive path following-AAR control strategy, the cost function of AS J_s, which is similar with Equation (13) and the cost function of AARR J_r, which mainly aims to improve roll stability of heavy vehicle during cornering, should be given firstly

$$\begin{aligned}J_i(N_p,k)&=\sum_{l=0}^{N_p}g_l^i\left(\mathbf{\Psi}(k+l),\mathbf{u}_f(k),\mathbf{u}_r(k)\right)\\&=\frac{1}{2}\sum_{l=0}^{N_p}[\mathbf{\Psi}^T(k+l)\xi_i\mathbf{\Psi}(k+l)+\mathbf{u}_i^T(k)\mathbf{R}_{ii}\mathbf{u}_i(k)\\&\quad+\mathbf{u}_j^T(k)\mathbf{R}_{ij}\mathbf{u}_j(k)],\ k\in\mathbf{K};\\&\qquad i,j=s,r;\ i\neq j\end{aligned} \quad (18)$$

where $gl\,f$, $gr\,f$ are the utility function of AS and AARB, respectively and $\mathbf{R}_{ii}$, $\mathbf{R}_{ij}$ $(i,j=s,r,\ i\neq j)$ are the weighting matrixes of control inputs of AS and AARB, and

$$\xi_s=\xi_{as},\xi_r=\mathbf{H}_r^T\mathbf{Q}_r\mathbf{H}_r,\mathbf{Q}_r=diag\left(\sigma_\phi\ \ \sigma_{Nf}\ \ \sigma_{Nr}\ \ \sigma_{\phi-\phi_{uf}}\ \ \sigma_{\phi-\phi_{ur}}\right)$$

$$\mathbf{H}_r=\begin{bmatrix}0&0&1&0&0&0&0&\cdots&0\\0&0&0&0&k_{tf}/F_{zf}l_w&0&0&\cdots&0\\0&0&0&0&0&k_{tr}/F_{zr}l_w&0&\cdots&0\\0&0&1&0&-1&0&0&\cdots&0\\0&0&1&0&0&-1&0&\cdots&0\end{bmatrix}_{5\times(8+2N_p)};$$

$$i,j=s,r;i\neq j$$

The LQ closed-loop feedback Nash interactive path following-AAR control strategy between AS and AARB system can be given by following *Corollary 1*.

Corollary 1: For the case of LQ dynamic games with strictly convex cost functionals, the feedback Nash solution can be determined in closed form as follows:

The path following-AAR LQ discrete-time dynamic game, as defined by (17) and (18), admits a unique feedback Nash solution which is linear in the current value of the state:

$$\mathbf{u}_i^*(k)=-\mathbf{L}_i(k)\mathbf{\Psi}(k),\quad k\in\mathbf{K};\ i=s,r \quad (19)$$

where $\mathbf{L}_i(k)$ satisfies the backward recurrence relation

$$\begin{aligned}&\mathbf{P}_s(k)=\left[\mathbf{A}_x-\mathbf{B}_s\mathbf{L}_s(k)-\mathbf{B}_r\mathbf{L}_r(k)\right]^T\mathbf{P}_s(k+1)\\&\times\left[\mathbf{A}_x-\mathbf{B}_s\mathbf{L}_s(k)-\mathbf{B}_r\mathbf{L}_r(k)\right]+\xi_s+\mathbf{L}_s^T(k)\mathbf{R}_{ss}\mathbf{L}_s(k)\\&\mathbf{P}_r(k)=\left[\mathbf{A}_x-\mathbf{B}_s\mathbf{L}_s(k)-\mathbf{B}_r\mathbf{L}_r(k)\right]^T\mathbf{P}_r(k+1)\\&\times\left[\mathbf{A}_x-\mathbf{B}_s\mathbf{L}_s(k)-\mathbf{B}_r\mathbf{L}_r(k)\right]+\xi_r+\mathbf{L}_r^T(k)\mathbf{R}_{ss}\mathbf{L}_r(k)\\&\mathbf{P}_s(N_p)=\xi_s,\mathbf{P}_r(N_p)=\xi_r\end{aligned} \quad (20)$$

where the relation between $\mathbf{L}_i(k)$ and $\mathbf{P}_i(k)$ can be expressed as

$$\begin{aligned}&\left[(\mathbf{B}_s)^T\mathbf{P}_s(k+1)\mathbf{B}_s+\mathbf{R}_{ss}\right]\mathbf{L}_s(k)\\&+(\mathbf{B}_s)^T\mathbf{P}_s(k+1)\mathbf{B}_r\mathbf{L}_r(k)=(\mathbf{B}_s)^T\mathbf{P}_s(k+1)\mathbf{A}_x\\&\left[(\mathbf{B}_r)^T\mathbf{P}_r(k+1)\mathbf{B}_r+\mathbf{R}_{rr}\right]\mathbf{L}_r(k)\\&+(\mathbf{B}_r)^T\mathbf{P}_r(k+1)\mathbf{B}_s\mathbf{L}_s(k)=(\mathbf{B}_r)^T\mathbf{P}_r(k+1)\mathbf{A}_x\end{aligned} \quad (21)$$

Proof: First, let system dynamic and performance index be defined by (17) and (18), with the following condition

$$\xi_i\geq 0,\mathbf{R}_{ii}\succ 0,\mathbf{R}_{ij}\geq 0\ \ \forall k\in\mathbf{K};\ i,j=s,r;i\neq j \quad (22)$$

Since our game solutions problem is limited in the LQ difference game situation, the following assumption for V_s and V_r holds

$$V_i(k+1,\mathbf{\Psi}(k+1))=\frac{1}{2}\mathbf{\Psi}^T(k+1)\mathbf{P}_i(k+1)\mathbf{\Psi}(k+1),\quad k\in\mathbf{K};\ i=s,r \quad (23)$$

Next, according to *Theorem 6.16* in [19] (pp. 320-322) and the strict convexity conditions given above, the feedback Nash equilibrium solution can be solved using the one-order necessary condition of optimality

$$\frac{\partial V_s\left(k,\Psi(k)\right)}{\partial \mathbf{u}_s(k)}=\frac{\partial V_r\left(k,\Psi(k)\right)}{\partial \mathbf{u}_r(k)}=0, k\in\mathbf{K}$$
$$\Leftrightarrow\begin{cases}\dfrac{\partial V_s\left(k+1,\Psi(k+1)\right)}{\partial\Gamma(k+1)}\dfrac{\partial f_k^s(\cdot)}{\partial \mathbf{u}_s(k)}+\dfrac{\partial \breve{g}_k^s(\cdot)}{\partial \mathbf{u}_s(k)}=0\\ \dfrac{\partial V_r\left(k+1,\Psi(k+1)\right)}{\partial\Gamma(k+1)}\dfrac{\partial f_k^r(\cdot)}{\partial \mathbf{u}_r(k)}+\dfrac{\partial \breve{g}_k^r(\cdot)}{\partial \mathbf{u}_r(k)}=0\end{cases} \quad (24)$$

Finally, according to (22), (23) (24) and after several algebraic operations, the backward recurrence relations and the control strategy solutions, which satisfy the feedback Nash equilibrium in *Corollary 1*, can be obtained. This completes the proof. ▪

$\mathscr{H}_\infty$ Optimal Control of Roll Stability for Autonomous Heavy Vehicle

As what mentioned above, the active anti-roll control strategy has been usually derived independent of front steering input, so for the purpose of comparison, a $\mathscr{H}_\infty$ optimal roll stability control strategy in which the AS input is only considered as the exogenous disturbance, is presented briefly.

Based on Equation (17) (meanwhile neglecting the white-noise reference signals $\mathbf{r}_{updata\ as}$ [10]) and regarding the AS inputs as the uncertain disturbances, the following uncertain discrete-time control model can be obtained

$$\begin{aligned}\Psi(k+1)&=\mathbf{A}_x\Psi(k)+\mathbf{B}\mathbf{u}(k)+\mathbf{D}\mathbf{w}(k)\\ \mathbf{z}(k)&=\mathbf{H}_k\Psi(k)+\mathbf{G}_k\mathbf{u}(k)\end{aligned} \quad (25)$$

where $\mathbf{u}(k)$ is the anti-roll control input, $\mathbf{w}(k)$ is the AS input disturbance and $\mathbf{z}(k)$ is the controlled output.

The control objective is: in a finite-time horizon (N_p), finding an admissible AAR controller yielding the closed-loop system with a finite L_2 gain less than or equal to a prescribed number γ.

$$\sum_{k=0}^{N_p}\left\|\mathbf{z}(k)\right\|^2\le\gamma^2\sum_{k=0}^{N_p}\left\|\mathbf{w}(k)\right\|^2,\ \forall\mathbf{w}(k)\in l^2\left(\left[0,N_p\right],\mathbb{R}^1\right) \quad (26)$$

The simplified derivation of AAR $\mathscr{H}_\infty$ roll stability control is given in the next section, the detailed description about this can be found in [20].

In order to derive the AAR $\mathscr{H}_\infty$ optimal roll stability control in the framework of zero-sum game theory [15, 20], the quadratic performance index should be given firstly

$$J_\gamma(\mathbf{u},\mathbf{w})=\sum_{k=0}^{N_p}\left\{\left|\Psi(k+1)\right|^2_{Q_{\gamma(k+1)}}+\left|\mathbf{u}(k)\right|^2_{R_{\gamma k}}\right\}\equiv\left\|\Psi\right\|^2_{Q_\gamma}+\left\|\mathbf{u}\right\|^2_{R_\gamma} \quad (27)$$

where $Q_{\gamma(k+1)}>0$, $R_{\gamma k}>0$ for all $k\in\mathbf{K}$, $|\bullet|_S$ denotes an appropriate Euclidean norm weighted by a nonnegative definite matrix S, and $\|\bullet\|$ denotes an appropriate (corresponding) l^2 norm. The disturbance attenuation problem can be described as: design a closed-loop controller $\mathbf{u}_\gamma$ which guarantees the maximum of J_γ less than or equal to the given attenuation level in all cases of energy bounded disturbances.

The problem of disturbance attenuation illustrated in (26) can be solved by the two players zero-sum differential game theory [15]. The basic idea behind this is: firstly, redefining a new cost functional (noted as NCF) which consists the performance and external disturbance index, then the control input aims to minimize such NCF while disturbance tries to maximize this, and finally, the dynamic programming method is used to derive the saddle point of NCF and the corresponding control input is the desired strategy.

Similar with [20], using the spirt of dynamic programming, the saddle point of NCF can be obtained by solving a sequence of static game.

Since the system dynamic model is linear and the NCF is the quadratic performance index, the unique saddle point solution of such disturbance attenuation problem can be given as [15, 20]

$$V_\gamma\left(k,\Psi(k)\right)=\frac{1}{2}\Psi^T(k)\mathbf{Z}(k)\Psi(k),\quad k\in\mathbf{K} \quad (28)$$

Using the principle of optimality, (28) can be solved by

$$\frac{\partial V_\gamma\left(k,\Psi(k)\right)}{\partial\mathbf{u}(k)}=\frac{\partial V_\gamma\left(k,\Psi(k)\right)}{\partial\mathbf{w}(k)}=0,\quad k\in\mathbf{K} \quad (29)$$

Considering the (25), (26), (27), (28), (29) and after several algebraic operation, the final optimal control strategy and the worst disturbance input can be expressed as the state feedback format and the detailed derivation and demonstration about this can be found in [20]

$$\begin{aligned}\mathbf{u}^*(k)&=-\mathbf{P}_u(k)\Psi(k)\\ \mathbf{w}^*(k)&=-\mathbf{P}_w(k)\Psi(k)\end{aligned} \quad (30)$$

It should be noted that the $\mathscr{H}_\infty$ optimal roll stability control is presented and discussed mainly for the purpose of comparing with interactive path following-AAR control strategy.

Simulation and Analysis

In this section, DLC driving scenario is used to verify the performance of the proposed method. The nonlinear Trucksim heavy vehicle evaluation model is adopted to evaluate the control strategy more practically and the nonlinearity mainly coming from the non-linear cornering phenomenon of tyre. Simulation results in three different control mode, namely without AAR (denoted as controller A), $\mathscr{H}_\infty$ optimal (denoted as controller B) and interactive path following-AAR control (denoted as controller C) are presented and compared with each other respectively. The detailed expression for ideal DLC and serpentine driving trajectories can be found in [14].

It should be noted that whether in the framework of interactive path following-AAR or $\mathscr{H}_\infty$ optimal control strategy, the selection of weighting matrixes, such as $\mathbf{Q}_\beta$, $\mathbf{Q}_r$ or $\mathbf{Q}_\gamma$, may result in different control performance [13, 14, 15]. In general, the large the performance weighting matrixes and the smaller the control input weighting matrixes are selected, the better

performance such as path following and roll stability will be obtained and simultaneously, the higher requirement, such as dynamic responses of high frequency for AS and AARB actuator should be satisfied. So, in order to validate the effectiveness of proposed control strategy in a fairer way, weighting matrixes which related to the path following control are selected as the same for controller A, B and C; weighting matrixes which related to the AAR control are selected as the same for controller B and C. All of these weights were chosen by iteratively tuning in simulation.

The DLC driving scenario which usually occur in normal lane change or emergency avoidance is performed to validate the proposed control strategy. The DLC maneuver has about 2.76m path deviation over 166.7m path longitudinal length. The forward velocity U is selected as 60km/h and under this setting the vehicle in controller A (without AAR control) will has rollover accident during the maneuver and the absolute value of its N_f or N_r is above 1 (as shown in Fig. 4b). It should be noted that the yaw-roll dynamic model of heavy vehicle is only valid if both the absolute value of N_f and N_r are below 1.

Fig. 4 shows the comparison of normalized load transfer at the front and rear axle under three different controllers. As shown in Fig. 4b, the value of N_r exceeds -1 at about 4.5s for controller A so that without anti-roll control, the rollover accident for heavy vehicle will occur. For controller B, compared with controller A, the maximum value of N_r and N_f can reduced effectively, respectively. So, it can be deduced that controller B can significantly enhance the roll stability of heavy vehicle in DLC maneuver.

FIGURE 4a Comparison of normalized load transfer at front axle (DLC)

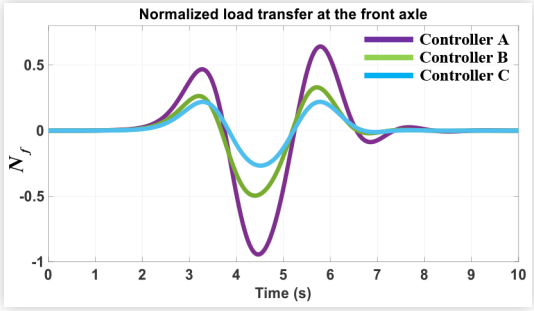

FIGURE 4b Comparison of normalized load transfer at rear axle (DLC)

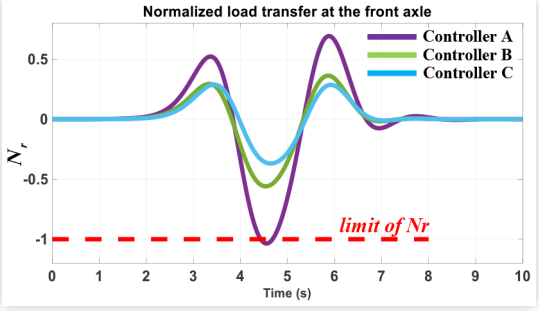

The most important results lie in the fact that, despite the same weighting matrixes are selected for controller B and C, compared with controller B, controller C can further make a reduction on N_r and N_β respectively, as shown in Fig. 4a and 4b. Therefore, the roll stability of heavy vehicle can be further guaranteed in interactive path following-AAR control strategy proposed in this paper. In the point of authors' view, the possible explanation for this finding is that unlike controller B in which the control input of AS is simply regarded as the exogenous disturbance in developing AAR control strategy, whereas there exists a certain interaction or communication between AS and AAR in developing their control strategies for controller C.

The AAR control torques comparisons at front and rear axle for controller B and C are shown in Fig. 5. It can be seen that compared with controller B, the large AAR control torques at front and rear axle will be exerted by controller C.

As what mentioned above, loss of control (rollover or lateral stability) during cornering is one of the main causes of heavy vehicle accidents. Therefore, it is necessary to evaluate the effects of three different controllers on the lateral stability of the heavy vehicle [6]. The vehicle stability region can be obtained from the phase plane (β-dβ/dt) and stability margin can be accessed through the stability index λ in Equation (31)

$$\lambda = \left| 2.49\dot{\beta} + 9.55\beta \right| \tag{31}$$

The heavy vehicle is in the stability region when λ<1 and the smaller the value of λ, the large lateral stability margin can be achieved. An advantage of controller C not to be neglected is the lateral stability aspect. As shown in Fig. 6, the stability index amplitude of controller B is smaller than that of A, while the stability index amplitude of C is smaller than that of B. Or in other words, during DLC maneuver, controller B can guarantee more lateral stability margin than A, controller C can guarantee more lateral stability margin than B. As shown in Equation (1)-(5), one possible explanation may be that there exists a certain coupling between lateral and roll dynamics of heavy vehicle.

The more pictorial descriptions of DLC maneuver of heavy vehicle for three different controllers are shown in Fig. 7. From Fig. 7, it can be seen that controller B presents smaller roll angle and smoother roll angle rate of sprung mass than that of A, controller C presents smaller roll angle and smoother roll angle rate of sprung mass than that of B. So, these results reflect the fact that the more roll stability margin can be obtained for controller C from the side.

FIGURE 5 Active anti-roll torque at front and rear axle (DLC)

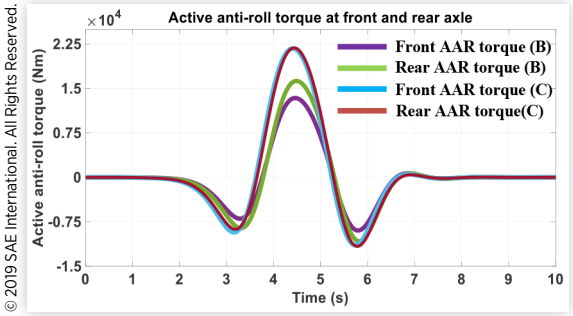

FIGURE 6 Stability index λ (DLC)

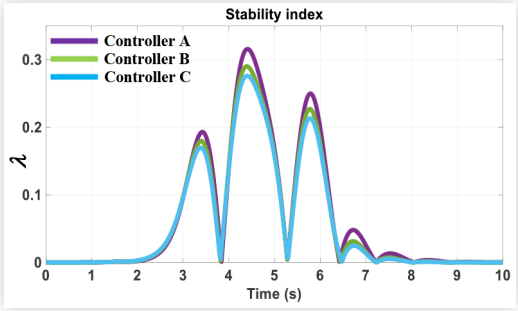

FIGURE 7 Double lane change maneuver (front view)

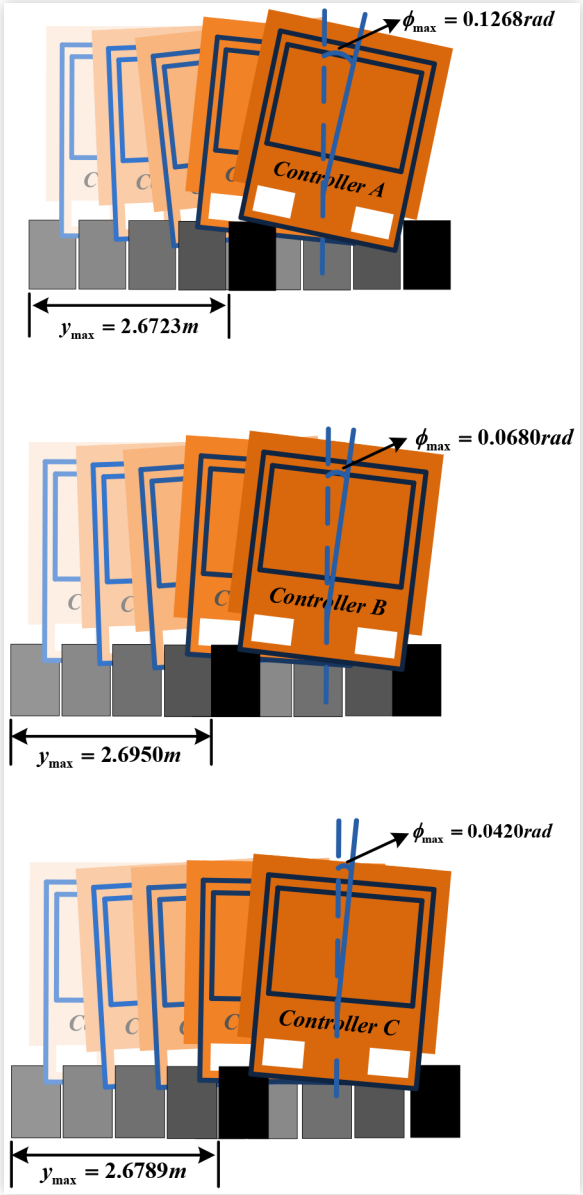

Overall, it can be concluded that though all three controllers can work well in terms of path following control, whereas, controller C proposed in this paper can give more roll stability as well as lateral stability margin than that of controller A and B during DLC maneuver. What's more, it can be naturally derived that when the heavy vehicle meets with the more emergency setting, e.g., emergency collision avoidance or serpentine driving scenario, compared with controller A and B, the proposed control method will provide more roll stability margin to avoid rollover accident.

Conclusion and Future Work

In this paper, the interactive and H_∞ optimal path following-AAR control strategies are developed and adopted to enhance roll stability of heavy vehicle during cornering. This study emphasizes the interests of the interactive path following-AAR control approach where based on dynamic game theory framework, the interactive control characteristics between AS and AAR system are considered directly in developing their respective control strategy. Simulation results show that the proposed control framework can significantly enhance vehicle roll stability as well as lateral stability meanwhile provide satisfied path tracking performance in DLC maneuver situations.

In future work, the dynamic behaviors of actuators such as electrically assisted hydraulic steering system will be considered in detailed in developing the interactive path following-AAR control strategy and furthermore based on rapid control prototyping (RCP) method and hardware-in-loop (HIL) implementation, the proposed path following-AAR control framework will be validated in real time.

References

1. Rath, J., Defoort, M., and Veluvlu, K., "Rollover Index Estimation in the Presence of Sensor Faluts, Unknown Inputs, and Uncertainties," *IEEE Trans. Intell. Transp. Syst.* 17(10):2949-2959, 2016.
2. Imine, H. and Djemai, M., "Switched Control for Reducing Impact of Vertical Forces on Road and Heavy-Vehicle Rollover Avoidance," *IEEE Trans Veh Technol.* 65(6):3499-3509, 2016.
3. Vu, V., Sename, O., Dugard, L., and Gaspar, P., "Enhancing Roll Stability of Heavy Vehicle by LQR Active Anti-Roll Bar Control Using Electronic Servo Valve Hydraulic Actuators," *Veh. Syst. Dyn.* 55(9):1405-1429, 2017.
4. Imine, H., Fridman, L., and Madani, T., "Steering Control for Rollover of Heavy Vehicle," *IEEE Trans Veh Technol.* 61(8):3499-3509, 2012.
5. Rajamani, R. and Piyabongkarn, D., "New Paradigms for the Integration of Yaw Stability and Rollover Prevention Functions in Vehicle Stability Control," *IEEE Trans. Intell. Transp. Syst.* 14(1):249-261, 2013.
6. Yim, S., Jeon, K., and Yi, K., "An Investigation into Vehicle Rollover Prevention by Coordinated Control of Active Anti-Roll Bar and Electronic Stability Program," *Int. J. Control. Autom. Syst* 10(2):275-297, 2012.

7. Gaspar, P., Szaszi, I., and bokor, J., "The Design of a Combined Control Structure to Prevent the Rollover of Heavy Vehicles," *Eur. J. Control* 10(2):148-162, 2004.
8. Ghazali, M., Durali, M., and Salarieh, H., "Path-Following in Model Predictive Rollover Prevention Using Front Steering and Braking," *Veh. Syst. Dyn.* 55(1):121-148, 2017.
9. Vu, V., Sename, O., Dugard, L., and Gaspar, P., "Active Anti-Roll Bar Control Using Electronic Servo Valve Hydraulic Damper on Single Unit Heavy Vehicle," in *8th IFAC Symposium on Advances in Automotive Control AAC 2016*, June 2016, Sweden, 20-23.
10. Tamaddoni, S.H., Taheri, S., and Ahmadian, M., "Optimal Preview Game Theory Approach to Vehicle Stability Controller Design," *Veh. Syst. Dyn.* 49(12):1967-1979, 2011.
11. Website:https://www.zf.com/corporate/en_de/products/product_range/commercial_vehicles/trucks_css_reax_gege_mounted.shtml.
12. Dextreit, C. and Kolmanovsky, I.V., "Game Theory Controller for Hybrid Electric Vehicles," *IEEE Trans. Control Syst. Technol.* 22(2):652-663, 2014.
13. Na, X. and Cole, D.J., "Game-Theoretic Modelling of the Steering Interaction between a Human Driver and a Vehicle Collision Avoidance Controller," *IEEE Trans. Hum. Mach. Syst.* 45(1):25-38, Feb. 2015.
14. Ji, X., Liu, Y., Na, X., and Liu, Y., "Research on Interactive Steering Control Strategy between Driver and AFS in Different Game Equilibrium Strategies and Information Patterns," *Veh. Syst. Dyn.* 56(9):1344-1374, 2018.
15. Ji, X., Liu, Y., He, X., Yang, K. et al., "Interactive Control Paradigm-Based Robust Lateral Stability Controller Design for Autonomous Automobile Path Tracking with Uncertain Disturbance: A Dynamic Game Approach," *IEEE Trans Veh Technol.* 67(8):6906-6920, 2018.
16. Sharp, R.S. and Valtetsiotis, V., "Optimal Preview Car Steering Control," *Veh. Syst. Dyn.* 35:101-117, 2001.
17. Sellami, Y., Imine, H., Boubezoul, A., and Cadiou, J., "Rollover Risk Prediction of Heavy Vehicles by Reliability Index and Empirical Modelling," *Veh. Syst. Dyn.* 56(3):385-405, 2018.
18. Morrison, G. and Cebon, D., "Combined Emergency Braking and Turning of Articulated Heavy Vehicles," *Veh. Syst. Dyn.* 55(5):725-749, 2017.
19. Basar, T. and Olsder, G.J., *Dynamic Noncooperative Game Theory* Second Edition (New York, USA: Academic Press, 1995).
20. Basar, T. and Bernhard, P., *H Optimal Control and Related Minimax Design Problem: A Dynamic Game Approach* (Boston, MA, USA: Birkhauser, 1991).

Contact Information

Dr. Liu, Yulong
State Key Laboratory of Automotive Safety and Energy, Tsinghua University, Beijing, China
Liuyl16@mails.tsinghua.edu.cn

Prof. Ji, Xuewu
State Key Laboratory of Automotive Safety and Energy, Tsinghua University, Beijing, China
jixw@mail.tsinghua.edu.cn

Acknowledgments

This paper is supported by the Natural Science Foundation of China [project no. U1664263, 51375009 and 51875302].

Appendix

$$\mathbf{A}_v = \mathbf{E}^{-1}\mathbf{A}_0, \mathbf{B}_\delta = \mathbf{E}^{-1}\mathbf{B}_0, \mathbf{B}_\mathbf{T} = \mathbf{E}^{-1}\mathbf{B}_1$$

$$\mathbf{E} = \begin{bmatrix} mU & 0 & 0 & -m_s h & 0 & 0 \\ 0 & I_{zz} & 0 & -I_{xz} & 0 & 0 \\ -m_s U h & -I_{xz} & 0 & I_{xx} + m_s h^2 & -b_f & -b_r \\ -m_{uf} U\left(r - h_{uf}\right) & 0 & 0 & 0 & b_f & 0 \\ -m_{ur} U\left(r - h_{ur}\right) & 0 & 0 & 0 & 0 & b_r \\ 0 & 0 & 1 & 0 & \mathbf{0} & 0 \end{bmatrix}$$

$$\mathbf{A_0} = \begin{bmatrix} Y_\beta & Y_{\dot\psi} - mU & 0 & 0 & 0 & 0 \\ N_\beta & N_{\dot\psi} & 0 & 0 & 0 & 0 \\ 0 & m_s U h & m_s g h - k_f - k_r & -\left(b_f + b_r\right) & k_f & k_r \\ -rC_f & m_{uf} U\left(r - h_{uf}\right) + rY_{\dot\psi f} & k_f & b_f & P_{kf} & 0 \\ -rC_r & m_{ur} U\left(r - h_{ur}\right) + rY_{\dot\psi r} & k_r & b_r & 0 & P_{kr} \\ 0 & 0 & 0 & 1 & 0 & 0 \end{bmatrix}$$

$$\mathbf{B_0} = \begin{bmatrix} Y_\delta & N_\delta & 0 & rY_\delta & 0 & 0 \end{bmatrix}^T, \mathbf{B_1} = \begin{bmatrix} 0 & 0 & 1 & 1 & 0 & 0 \\ 0 & 0 & 1 & 0 & 1 & 0 \end{bmatrix}^T, \mathbf{T} = \begin{bmatrix} T_f & T_r \end{bmatrix}^T$$

$$Y_{\dot\psi f} = -\frac{l_f C_f}{U}, Y_{\dot\psi r} = \frac{l_r C_r}{U}, P_{kf} = m_{uf} g h_{uf} - k_f - k_{tf}, P_{kr} = m_{ur} g h_{ur} - k_r - k_{tr}$$

ISSN 0148-7191